Electronic Research Archive

http://www.aimspress.com/journal/era

ERA, 31(6): 3145–3168.
DOI: 10.3934/era.2023159
Received: 17 November 2022
Revised: 28 February 2023
Accepted: 06 March 2023
Published: 23 March 2023

Research article

High-order compact difference methods for solving two-dimensional nonlinear wave equations

Shuaikang Wang[1], **Yunzhi Jiang**[2] **and Yongbin Ge**[1,*]

[1] Institute of Applied Mathematics and Mechanics, Ningxia University, Yinchuan, China

[2] Basic Courses Teaching and Research Department, Yingkou Institute of Technology, Yingkou, China

* **Correspondence:** Email: gybnxu@yeah.net.

Abstract: Nonlinear wave equations are widely used in many areas of science and engineering. This paper proposes two high-order compact (HOC) difference schemes with convergence orders of $O\left(\tau^4 + h_x^4 + h_y^4\right)$ that can be used to solve nonlinear wave equations. The first scheme is a nonlinear compact difference scheme with three temporal levels. After calculating the second-order spatial derivatives of the previous time level using the Padé scheme, numerical solutions of the next time level are obtained through repeated iterations. The second scheme is a three-level linearized compact difference scheme. Unlike the first scheme, iterations are not required and it obtains numerical solutions through an explicit calculation. The two proposed schemes are applied to solutions of the coupled sine-Gordon equations. Finally, some numerical experiments are presented to confirm the effectiveness and accuracy of the proposed schemes.

Keywords: nonlinear wave equation; nonlinear compact difference scheme; three-level linearized compact difference scheme; coupled sine-Gordon equations

1. Introduction

Nonlinear wave equations are used in various fields of science and engineering, such as quantum field theory, nonlinear optics, fluid mechanics, and so on [1–3]. As the mathematical models of many complex real-world phenomena involve coefficients that vary in time and space [4, 5], this paper considers the following two-dimensional nonlinear wave equation with variable coefficients:

$$\frac{\partial^2 u}{\partial t^2} = v^2(x,y)\left(\frac{\partial^2 u}{\partial x^2} + \frac{\partial^2 u}{\partial y^2}\right) + f(u,x,y,t), \quad (x,y,t) \in \Omega \times (0,T], \tag{1.1}$$

in which $\Omega = [a_1, b_1] \times [a_2, b_2]$ and $a_i, b_i \in \mathbb{R}\,(i = 1, 2)$. The initial conditions are given as

$$u(x,y,0)=\varphi(x,y),\quad \frac{\partial u(x,y,0)}{\partial t}=\psi(x,y),\qquad (x,y)\in\Omega, \tag{1.2}$$

and the boundary conditions are

$$u(a_1,y,t)=g_0(y,t),\ u(b_1,y,t)=g_1(y,t),\qquad (y,t)\in[a_2,b_2]\times(0,T], \tag{1.3a}$$
$$u(x,a_2,t)=l_0(x,t),\ u(x,b_2,t)=l_1(x,t),\qquad (x,t)\in[a_1,b_1]\times(0,T], \tag{1.3b}$$

or the periodic boundary conditions are

$$u(x,y,t)=u(x+L_1,y,t),\qquad (x,y,t)\in\Omega\times(0,T], \tag{1.4a}$$
$$u(x,y,t)=u(x,y+L_2,t),\qquad (x,y,t)\in\Omega\times(0,T], \tag{1.4b}$$

where $L_1=b_1-a_1$, $L_2=b_2-a_2$, $v(x,y)$ is the acoustic velocity and $f(u,x,y,t)$ is a nonlinear expressions in terms of u. Assume that $\varphi(x,y)$, $\phi(x,y)$, $g_0(y,t)$, $g_1(y,t)$, $l_0(x,t)$ and $l_1(x,t)$ are smooth known functions.

When $v(x,y)=1$ and the nonlinear term $f(u,x,y,t)$ is a polynomial with respect to u, $-sinh(u)$, or $-sin(u)$, Eq (1.1) can be simplified to the corresponding Klein–Gordon equation, sinh–Gordon equation, or sine–Gordon equation [6]. These equations embody different nonlinear physical phenomena. Soliton waves, which is one of the most conspicuous solutions to the sine-Gordon and Klein-Gordon equations, occur in many physical processes [7]. In addition, Khusnutdinova and Pelinovsky [8] derived the coupled sine–Gordon equations reflecting certain physical and biological phenomena [9–11].

The widespread use of nonlinear wave equations has led to strong interest in their solutions. In the past decades, analytical solutions to problems with special initial boundary value conditions have been obtained using various analytical methods [12–15]. In addition, researchers have investigated the corresponding Cauchy problem and the properties of soliton solutions [16–18]. However, it is not possible to obtain analytical solutions to problems with arbitrary initial boundary value conditions. Thus, different numerical methods have been developed to solve nonlinear wave equations, such as finite difference methods [6,19–22], differential quadrature methods [3], finite element methods [23,24] and predictor-corrector schemes [25,26], etc.

In recent years, various high-order compact schemes have been used to solve nonlinear wave equations. In [19], two high-order compact alternating direction implicit (ADI) schemes with truncation errors of $O\left(\tau^2+h^4\right)$ have been proposed for the generalized sine–Gordon equation. One of them is a nonlinear scheme and the other is a linear scheme. A three-level compact ADI scheme with second-order convergence in the time direction and fourth-order convergence in space has been used to solve nonlinear wave equations [21], and the time accuracy can be increased to the fourth order through an extrapolation formula. Two- and three-level compact ADI schemes have been presented for solving the two-dimensional telegraph equations with nonlinear forcing [20]. Deng and Zhang [27] derived a compact multi-step ADI scheme to solve the nonlinear viscous wave equation by combining the second-order backward differential formula and the fourth-order Padé approximation, and finally applied a three-level Richardson extrapolation algorithm to reach fourth-order accuracy in the time direction. Deng [28] proposed two ADI schemes with convergence orders of $O\left(\tau^2+h^4\right)$ for solving nonlinear wave equations containing a viscous term. Deng and Liang [6] presented two compact ADI

schemes with truncation errors of $O\left(\tau^4 + h^4\right)$ for nonlinear wave equations. One of them is nonlinear and involves three temporal levels, while the other is a five-level linear scheme. In [22], an energy-preserving average vector field compact difference scheme for nonlinear wave equations is described. This achieves fourth-order convergence in different directions. For the coupled nonlinear sine–Gordon equations, various numerical methods have been proposed in recent years. A numerical simulation method is proposed in [29], while Deng [30] established a high-order compact ADI scheme by combining the fourth-order compact difference operator and the Crank–Nicolson method. The coupled nonlinear sine–Gordon equations are solved by two compact ADI schemes in [6].

The existing finite difference schemes for solving two-dimensional nonlinear wave equations are typically based on the ADI method. At present, some schemes only have second-order convergence in the time direction, while other schemes have fourth-order convergence in both the temporal and spatial dimensions, but their computational efficiency is relatively poor. Explicit difference schemes offer high computational efficiency in solving partial differential equations [31–33]. Therefore, it is a challenging task to construct numerical methods with high temporal and spatial accuracy, and higher computational efficiency. So, in order to improve computational efficiency, this paper presents two high-order compact difference schemes based on the explicit difference approach. The remainder of this paper is structured as follows. In Section 2, two high-order compact (HOC) difference schemes for solving the nonlinear wave equation are presented. In Section 3, two high-order difference schemes are employed to simulate the coupled sine–Gordon equations. In Section 4, we present five numerical examples to verify the effectiveness and accuracy of the proposed HOC schemes. The conclusions to this study are presented in Section 5.

2. HOC difference schemes

In this section, two HOC difference schemes for simulating the nonlinear system of (1.1)–(1.4) are derived. First, we give some definitions and a lemma that will be useful in constructing the HOC difference schemes. We consider the domain $[a_1, b_1] \times [a_2, b_2] \times (0, T]$, in which $[a_1, b_1]$ is divided into M_x uniform intervals, $a_1 = x_0 < x_1 < x_2 < \cdots < x_{M_x} = b_1$, $[a_2, b_2]$ is divided into M_y uniform intervals, $a_2 = y_0 < y_1 < y_2 < \cdots < y_{M_y} = b_2$, and $(0, T]$ is divided into N uniform intervals. The spatial steps are $h_x = \frac{b_1 - a_1}{M_x}$ and $h_y = \frac{b_2 - a_2}{M_y}$, and the time step is $\tau = \frac{T}{N}$. Denoting each mesh point as (x_i, y_j, t_n), $x_i = a_1 + ih_x, y_j = a_2 + jh_y, t_n = n\tau$, $i = 0, 1, \cdots, M_x$, $j = 0, 1, \cdots, M_y$, $n = 0, 1, \cdots, N$.

We denote $\Omega_\tau = \{t_n | 0 \le n \le N\}$, $\Omega_h = \{(x_i, y_j) | 0 \le i \le M_x, 0 \le j \le M_y\}$, $\Omega_{h\tau} = \Omega_h \times \Omega_\tau$. Define the grid function $v = \{v_{i,j}^n | 0 \le i \le M_x, 0 \le j \le M_y, 0 \le n \le N\}$ on $\Omega_{h\tau}$, and denote

$$\delta_x^2 v_{i,j}^n = \frac{1}{h_x^2}(v_{i+1,j}^n - 2v_{i,j}^n + v_{i-1,j}^n), \delta_y^2 v_{i,j}^n = \frac{1}{h_y^2}(v_{i,j+1}^n - 2v_{i,j}^n + v_{i,j-1}^n), \delta_t^2 v_{i,j}^n = \frac{1}{\tau^2}(v_{i,j}^{n+1} - 2v_{i,j}^n + v_{i,j}^{n-1}).$$

Lemma 1. *[6] Suppose that $q(t) \in C^4(I)$, $t \in I$. Then, we have $q(t_{n+1}) = 4q(t_n) - 6q(t_{n-1}) + 4q(t_{n-2}) - q(t_{n-3}) + O\left(\Delta t^4\right)$, where $\Delta t = t_{n+k} - t_{n+k-1}, (k = -2, -1, 0, \text{ or } 1)$.*

This section focuses on the construction of HOC difference schemes for the problem with Dirichlet boundary conditions (1.3).

2.1. HOC scheme for the start-up time step

Let $\vartheta(x, y) = v^2(x, y)$. Equation (1.1) can be rewritten as

$$\frac{\partial^2 u}{\partial t^2} = \vartheta(x,y)\left(\frac{\partial^2 u}{\partial x^2} + \frac{\partial^2 u}{\partial y^2}\right) + f(u,x,y,t). \tag{2.1}$$

First, using the Taylor series expansion at the grid nodes $\left(x_i, y_j, t_0\right)$ yields

$$u_{i,j}^1 = u_{i,j}^0 + \sum_{k=1}^{4} \frac{\tau^k}{k!}\frac{\partial^k u}{\partial t^k}\left(x_i, y_j, 0\right) + O\left(\tau^5\right), \quad 0 \le i \le M_x, 0 \le j \le M_y. \tag{2.2}$$

According to Eqs (1.1) and (1.2), $\frac{\partial^2 u}{\partial t^2}\left(x_i, y_j, 0\right)$, $\frac{\partial^3 u}{\partial t^3}\left(x_i, y_j, 0\right)$, and $\frac{\partial^4 u}{\partial t^4}\left(x_i, y_j, 0\right)$ can be easily calculated. For simplicity, we denote $f\left(u_{i,j}^n, x_i, y_j, t_n\right) := f\left(u_{i,j}^n\right)$. Considering $\varphi\left(x_i, y_j\right)$, $\psi\left(x_i, y_j\right)$ and (2.2), the following high-order approximation for $u\left(x_i, y_j, \tau\right)$ can be obtained:

$$\begin{aligned} u_{i,j}^1 = {} & \varphi_{i,j} + \tau\psi_{i,j} + \frac{\tau^2}{2}\left[\vartheta_{i,j}\left(\varphi_{xx} + \varphi_{yy}\right)_{i,j} + f\left(\varphi_{i,j}\right)\right] + \frac{\tau^3}{6}\left[\vartheta_{i,j}\left(\psi_{xx} + \psi_{yy}\right)_{i,j} + f_t\left(\varphi_{i,j}\right)\right] \\ & + \frac{\tau^4\vartheta_{i,j}}{24}\left[f_{xx}\left(\varphi_{i,j}\right) + f_{yy}\left(\varphi_{i,j}\right) + \left(\vartheta_{xx} + \vartheta_{yy}\right)_{i,j}\left(\varphi_{xx} + \varphi_{yy}\right)_{i,j} + \vartheta_{i,j}\left(\varphi_{xxxx} + \varphi_{yyyy}\right)_{i,j}\right] \\ & + \frac{\tau^4\vartheta_{i,j}}{12}\left[(\vartheta_x)_{i,j}\left(\varphi_{xxx} + \varphi_{xyy}\right)_{i,j} + \left(\vartheta_y\right)_{i,j}\left(\varphi_{xxy} + \varphi_{yyy}\right)_{i,j} + \vartheta_{i,j}\left(\varphi_{xxyy}\right)_{i,j}\right] + \frac{\tau^4}{24} f_{tt}\left(\varphi_{i,j}\right), \end{aligned} \tag{2.3}$$

in which $f_t\left(\varphi_{i,j}\right)$ and $f_{tt}\left(\varphi_{i,j}\right)$ can be obtained by the chain rule as

$$\frac{\partial f}{\partial t}\left(\varphi_{i,j}, x_i, y_j, 0\right) = \frac{\partial f}{\partial t}\left(\varphi_{i,j}, x_i, y_j, 0\right) + \left(\frac{\partial u}{\partial t}\right)_{i,j}^0 \frac{\partial f}{\partial u}\left(\varphi_{i,j}, x_i, y_j, 0\right), \tag{2.4}$$

$$\begin{aligned} \frac{\partial^2 f}{\partial t^2}\left(\varphi_{i,j}, x_i, y_j, 0\right) = {} & \frac{\partial^2 f}{\partial t^2}\left(\varphi_{i,j}, x_i, y_j, 0\right) + 2\left(\frac{\partial u}{\partial t}\right)_{i,j}^0 \frac{\partial^2 f}{\partial u \partial t}\left(\varphi_{i,j}, x_i, y_j, 0\right) \\ & + \left(\frac{\partial^2 u}{\partial t^2}\right)_{i,j}^0 \frac{\partial f}{\partial u}\left(\varphi_{i,j}, x_i, y_j, 0\right) + \left[\left(\frac{\partial u}{\partial t}\right)_{i,j}^0\right]^2 \frac{\partial^2 f}{\partial u^2}\left(\varphi_{i,j}, x_i, y_j, 0\right). \end{aligned} \tag{2.5}$$

2.2. HOC difference scheme for the other time steps

For the discretization of $\frac{\partial^2 u}{\partial t^2}$, the central difference with truncated remainders yields

$$\left(\frac{\partial^2 u}{\partial t^2}\right)_{i,j}^n = \delta_t^2 u_{i,j}^n - \frac{\tau^2}{12}\left(\frac{\partial^4 u}{\partial t^4}\right)_{i,j}^n + \left(R_t\right)_{i,j}^n, \quad 0 \le i \le M_x, 0 \le j \le M_y, 1 \le n \le N-1, \tag{2.6}$$

where $\left(R_t\right)_{i,j}^n = O\left(\tau^4\right)$. According to Eq (2.1), we have

$$\begin{aligned} \frac{\partial^4 u}{\partial t^4} = \frac{\partial^2}{\partial t^2}\left(\frac{\partial^2 u}{\partial t^2}\right) &= \frac{\partial^2}{\partial t^2}\left[\vartheta(x,y)\left(\frac{\partial^2 u}{\partial x^2} + \frac{\partial^2 u}{\partial y^2}\right) + f(u,x,y,t)\right] \\ &= \vartheta(x,y)\left[\frac{\partial^2}{\partial x^2}\left(\frac{\partial^2 u}{\partial t^2}\right) + \frac{\partial^2}{\partial y^2}\left(\frac{\partial^2 u}{\partial t^2}\right)\right] + \frac{\partial^2 f(u,x,y,t)}{\partial t^2}. \end{aligned} \tag{2.7}$$

Substituting (2.7) into (2.6) and discretizing the spatial derivatives with the central difference operator, we obtain

$$\left(\frac{\partial^2 u}{\partial t^2}\right)_{i,j}^n = \delta_t^2 u_{i,j}^n - \frac{\vartheta_{i,j}\tau^2}{12}\left[\delta_x^2\left(\frac{\partial^2 u}{\partial t^2}\right)_{i,j}^n + \delta_y^2\left(\frac{\partial^2 u}{\partial t^2}\right)_{i,j}^n\right] - \frac{\tau^2}{12}\frac{\partial^2 f\left(u_{i,j}^n\right)}{\partial t^2} + (R_1)_{i,j}^n, \tag{2.8}$$
$$1 \le i \le M_x - 1, 1 \le j \le M_y - 1, 1 \le n \le N - 1,$$

in which $(R_1)_{i,j}^n = O\left(\tau^4 + \tau^2 h_x^2 + \tau^2 h_y^2\right)$.

Substituting $\frac{\partial^2 u}{\partial t^2}$ into the above formula with Eq (2.1) gives

$$\begin{aligned}\delta_t^2 u_{i,j}^n = {} & \vartheta_{i.j}\left(\frac{\partial^2 u}{\partial x^2} + \frac{\partial^2 u}{\partial y^2}\right)_{i,j}^n + f\left(u_{i,j}^n\right) + \frac{\vartheta_{i,j}\tau^2}{12}\left\{\delta_x^2\left[\vartheta_{i,j}\left(\frac{\partial^2 u}{\partial x^2} + \frac{\partial^2 u}{\partial y^2}\right)_{i,j}^n + f\left(u_{i,j}^n\right)\right]\right. \\ & \left. + \delta_y^2\left[\vartheta_{i,j}\left(\frac{\partial^2 u}{\partial x^2} + \frac{\partial^2 u}{\partial y^2}\right)_{i,j}^n + f\left(u_{i,j}^n\right)\right]\right\} + \frac{\tau^2}{12}\frac{\partial^2 f\left(u_{i,j}^n\right)}{\partial t^2} + (R_1)_{i,j}^n.\end{aligned} \tag{2.9}$$

Then, $\frac{\partial^2 f\left(u_{i,j}^n\right)}{\partial t^2}$ is discretized using the central difference scheme. Rearranging (2.9) and neglecting the truncation error, we have the HOC difference scheme

$$\begin{aligned}\delta_t^2 u_{i,j}^n = {} & \left(1 + \frac{\vartheta_{i,j}\tau^2}{12}\delta_x^2 + \frac{\vartheta_{i,j}\tau^2}{12}\delta_y^2\right)\left[\vartheta_{i.j}\left(\frac{\partial^2 u}{\partial x^2}\right)_{i,j}^n\right] + \left(1 + \frac{\vartheta_{i,j}\tau^2}{12}\delta_x^2 + \frac{\vartheta_{i,j}\tau^2}{12}\delta_y^2\right)\left[\vartheta_{i.j}\left(\frac{\partial^2 u}{\partial y^2}\right)_{i,j}^n\right] \\ & + \left(1 + \frac{\vartheta_{i,j}\tau^2}{12}\delta_x^2 + \frac{\vartheta_{i,j}\tau^2}{12}\delta_y^2\right) f\left(u_{i,j}^n\right) + \frac{1}{12}\left[f\left(u_{i,j}^{n+1}\right) - 2f\left(u_{i,j}^n\right) + f\left(u_{i,j}^{n-1}\right)\right],\end{aligned} \tag{2.10}$$

which we call HOC-I for convenience. Letting $\lambda_x = \frac{\tau}{h_x}$ and $\lambda_y = \frac{\tau}{h_y}$, HOC-I scheme can be rewritten as

$$\begin{aligned}u_{i,j}^{n+1} = {} & 2u_{i,j}^n - u_{i,j}^{n-1} + \left(\vartheta_{i,j}\tau^2 - \frac{\vartheta_{i,j}^2\tau^2\lambda_x^2}{6} - \frac{\vartheta_{i,j}^2\tau^2\lambda_y^2}{6}\right)\left[\left(\frac{\partial^2 u}{\partial x^2}\right)_{i,j}^n + \left(\frac{\partial^2 u}{\partial y^2}\right)_{i,j}^n\right] \\ & + \frac{\vartheta_{i,j}\tau^2\lambda_x^2}{12}\left[\vartheta_{i+1,j}\left(\frac{\partial^2 u}{\partial x^2}\right)_{i+1,j}^n + \vartheta_{i-1,j}\left(\frac{\partial^2 u}{\partial x^2}\right)_{i-1,j}^n + \vartheta_{i+1,j}\left(\frac{\partial^2 u}{\partial y^2}\right)_{i+1,j}^n + \vartheta_{i-1,j}\left(\frac{\partial^2 u}{\partial y^2}\right)_{i-1,j}^n\right] \\ & + \frac{\vartheta_{i,j}\tau^2\lambda_y^2}{12}\left[\vartheta_{i,j+1}\left(\frac{\partial^2 u}{\partial x^2}\right)_{i,j+1}^n + \vartheta_{i,j-1}\left(\frac{\partial^2 u}{\partial x^2}\right)_{i,j-1}^n + \vartheta_{i,j+1}\left(\frac{\partial^2 u}{\partial y^2}\right)_{i,j+1}^n + \vartheta_{i,j-1}\left(\frac{\partial^2 u}{\partial y^2}\right)_{i,j-1}^n\right] \\ & + \left(\tau^2 - \frac{\vartheta_{i,j}\tau^2\lambda_x^2}{6} - \frac{\vartheta_{i,j}\tau^2\lambda_y^2}{6}\right) f\left(u_{i,j}^n\right) + \frac{\vartheta_{i,j}\tau^2\lambda_x^2}{12}\left[f\left(u_{i+1,j}^n\right) + f\left(u_{i-1,j}^n\right)\right] \\ & + \frac{\vartheta_{i,j}\tau^2\lambda_y^2}{12}\left[f\left(u_{i,j+1}^n\right) + f\left(u_{i,j-1}^n\right)\right] + \frac{\tau^2}{12}\left[f\left(u_{i,j}^{n+1}\right) - 2f\left(u_{i,j}^n\right) + f\left(u_{i,j}^{n-1}\right)\right].\end{aligned} \tag{2.11}$$

Remark 1: For nonlinear wave equations with periodic boundaries (1.4), there is $U_{i,j}^n = U_{i+M_x,j}^n$ for $i \le 0$, $U_{i,j}^n = U_{i,j+M_y}^n$ for $j \le 0$, $U_{i,j}^n = U_{i-M_x,j}^n$ for $i > M_x$ and $U_{i,j}^n = U_{i,j-M_y}^n$ for $j > M_y$. At the same time, the grid point range $\left\{\left(x_i, y_j, t_n\right) | 1 \le i \le M_x, 1 \le j \le M_y, 1 \le n \le N - 1\right\}$ for high-order scheme (2.11) calculations.

Obviously, we note that the calculation of HOC-I requires the values of $\left(\frac{\partial^2 U}{\partial x^2}\right)_{i,j}^n$ and $\left(\frac{\partial^2 U}{\partial y^2}\right)_{i,j}^n$ to be known. These can be calculated by the following fourth-order Padé schemes [34]:

$$\left(\frac{\partial^2 u}{\partial x^2}\right)_{i+1,j}^n + 10\left(\frac{\partial^2 u}{\partial x^2}\right)_{i,j}^n + \left(\frac{\partial^2 u}{\partial x^2}\right)_{i-1,j}^n = 12\frac{u_{i+1,j}^n - 2u_{i,j}^n + u_{i-1,j}^n}{h_x^2} + O\left(h_x^4\right), \tag{2.12}$$

$$1 \le i \le M_x - 1,\ 0 \le j \le M_y,\ 1 \le n \le N - 1,$$

$$\left(\frac{\partial^2 u}{\partial y^2}\right)_{i,j+1}^n + 10\left(\frac{\partial^2 u}{\partial y^2}\right)_{i,j}^n + \left(\frac{\partial^2 u}{\partial y^2}\right)_{i,j-1}^n = 12\frac{u_{i,j+1}^n - 2u_{i,j}^n + u_{i,j-1}^n}{h_y^2} + O\left(h_y^4\right), \tag{2.13}$$

$$0 \le i \le M_x,\ 1 \le j \le M_y - 1,\ 1 \le n \le N - 1,$$

where the boundaries can be calculated exactly by the following formulas:

$$\begin{aligned}\left(\frac{\partial^2 u}{\partial x^2}\right)_{0,j}^n &= \frac{1}{\vartheta_{0,j}}\left[\frac{\partial^2 u}{\partial t^2} - f(u)\right]_{0,j}^n - \left(\frac{\partial^2 u}{\partial y^2}\right)_{0,j}^n \\ &= \frac{1}{\vartheta_{0,j}}\left[\frac{\partial^2 g_0}{\partial t^2} - f(u)\right]_{0,j}^n - \left(\frac{\partial^2 g_0}{\partial y^2}\right)_{0,j}^n, \quad j = 0, 1, \cdots, M_y,\end{aligned} \tag{2.14}$$

$$\begin{aligned}\left(\frac{\partial^2 u}{\partial x^2}\right)_{M_x,j}^n &= \frac{1}{\vartheta_{M_x,j}}\left[\frac{\partial^2 u}{\partial t^2} - f(u)\right]_{M_x,j}^n - \left(\frac{\partial^2 u}{\partial y^2}\right)_{M_x,j}^n \\ &= \frac{1}{\vartheta_{M_x,j}}\left[\frac{\partial^2 g_1}{\partial t^2} - f(u)\right]_{M_x,j}^n - \left(\frac{\partial^2 g_1}{\partial y^2}\right)_{M_x,j}^n, \quad j = 0, 1, \cdots, M_y,\end{aligned} \tag{2.15}$$

$$\begin{aligned}\left(\frac{\partial^2 u}{\partial y^2}\right)_{i,0}^n &= \frac{1}{\vartheta_{i,0}}\left[\frac{\partial^2 u}{\partial t^2} - f(u)\right]_{i,0}^n - \left(\frac{\partial^2 u}{\partial x^2}\right)_{i,0}^n \\ &= \frac{1}{\vartheta_{i,0}}\left[\frac{\partial^2 l_0}{\partial t^2} - f(u)\right]_{i,0}^n - \left(\frac{\partial^2 l_0}{\partial x^2}\right)_{i,0}^n, \quad i = 0, 1, \cdots, M_x,\end{aligned} \tag{2.16}$$

$$\begin{aligned}\left(\frac{\partial^2 u}{\partial y^2}\right)_{i,M_y}^n &= \frac{1}{\vartheta_{i,M_y}}\left[\frac{\partial^2 u}{\partial t^2} - f(u)\right]_{i,M_y}^n - \left(\frac{\partial^2 u}{\partial x^2}\right)_{i,M_y}^n \\ &= \frac{1}{\vartheta_{i,M_y}}\left[\frac{\partial^2 l_1}{\partial t^2} - f(u)\right]_{i,M_y}^n - \left(\frac{\partial^2 l_1}{\partial x^2}\right)_{i,M_y}^n, i = 0, 1, \cdots, M_x.\end{aligned} \tag{2.17}$$

Noting that the two coefficient matrices constituted by (2.12)–(2.17) are all tridiagonal matrices, so we can efficiently solve these linear systems using the Thomas algorithm.

Remark 2: For nonlinear problems with periodic boundaries (1.4), $\left(\frac{\partial^2 u}{\partial x^2}\right)_{i,j}^n$ and $\left(\frac{\partial^2 u}{\partial y^2}\right)_{i,j}^n$ can be calculated directly through (2.12) and (2.13) without calculating boundaries (2.14)–(2.17). The coefficient matrices can be written as

$$\begin{bmatrix} 10 & 1 & & & 1 \\ 1 & 10 & 1 & & \\ & \ddots & \ddots & \ddots & \\ & & 1 & 10 & 1 \\ 1 & & & 1 & 10 \end{bmatrix}_{M_x \times M_x} \qquad \begin{bmatrix} 10 & 1 & & & 1 \\ 1 & 10 & 1 & & \\ & \ddots & \ddots & \ddots & \\ & & 1 & 10 & 1 \\ 1 & & & 1 & 10 \end{bmatrix}_{M_y \times M_y}$$

Similarly, we can solve these linear systems using Thomas algorithm for quasi-tridiagonal matrices.

In this way, we obtain the HOC-I difference scheme with a truncation error of $O\left(\tau^4+\tau^2h_x^2+\tau^2h_y^2+h_x^4+h_y^4\right)$ for solving Eqs (1.1)–(1.4). This scheme achieves fourth-order accuracy in both the temporal and spatial dimensions. We can apply HOC-I using Algorithm 1.

Algorithm 1:

Step 1 : $\left\{u_{i,j}^0|\left(x_i,y_j\right)\in\Omega_h\right\}$ *and* $\left\{u_{i,j}^1|\left(x_i,y_j\right)\in\Omega_h\right\}$ *can be calculated by* (1.2) *and* (2.3), *respectively*;

Step 2 : *Calculate* $\left(\frac{\partial^2u}{\partial x^2}\right)_{i,j}^n$ *and* $\left(\frac{\partial^2u}{\partial x^2}\right)_{i,j}^n$ *by* (2.12) − (2.17);

Step 3 : *Next*, $\left\{u_{i,j}^{n+1}|\left(x_i,y_j\right)\in\Omega_h\right\}$, $(n=1,\ 2,\ \cdots,\ N-1)$ *is calculated iteratively. Let* $u_{i,j}^{n+1,(0)}=0$.

(1) *Let* $u_{i,j}^{n+1,(k)}\leftarrow u_{i,j}^{n+1,(k-1)}$, *then calculate*$f\left(u_{i,j}^{n+1,(k)}\right)$, $f\left(u_{i,j}^n\right)$ *and* $f\left(u_{i,j}^{n-1}\right)$;

(2) *Calculate* $u_{i,j}^{n+1,(k)}$ *by* (2.11);

(3) *Let* $k-1\leftarrow k$, *repeat the above calculation process till* $\|u_{i,j}^{n+1,(k)}-u_{i,j}^{n+1,(k-1)}\|<\varepsilon$, *set* $u_{i,j}^{n+1}\leftarrow u_{i,j}^{n+1,(k)}$;

Step 4 : *Let* $n\leftarrow n+1$, *repeat the above Step* 2 *and Step* 3 *till the time reaches the final moment, and the calculation is terminated.*

[1] Note: k is iteration number and $k=1,\ 2,\ \cdots$.

Remark 3: In the Step 2 of Algorithm 1, $\left(\frac{\partial^2u}{\partial x^2}\right)_{i,j}^n$ and $\left(\frac{\partial^2u}{\partial y^2}\right)_{i,j}^n$ can be calculated directly through (2.12) and (2.13) for the problems with periodic boundaries.

2.3. Linearized HOC difference scheme

As the HOC-I scheme is nonlinear, multiple iterations are required at each time level, which increases the computation time. To avoid iterations and improve computational efficiency, we linearize the nonlinear term $f\left(u_{i,j}^{n+1}\right)$ of HOC-I to obtain a linear HOC scheme. According to Lemma 1, we have

$$f\left(u_{i,j}^{n+1}\right)=f\left(4u_{i,j}^n-6u_{i,j}^{n-1}+4u_{i,j}^{n-2}-u_{i,j}^{n-3}\right). \tag{2.18}$$

Substituting (2.18) into (2.10) gives the following linear HOC difference scheme:

$$\begin{aligned}\delta_t^2u_{i,j}^n=&\left(1+\frac{\vartheta_{i,j}\tau^2}{12}\delta_x^2+\frac{\vartheta_{i,j}\tau^2}{12}\delta_y^2\right)\left[\vartheta_{i.j}\left(\frac{\partial^2u}{\partial x^2}\right)_{i,j}^n\right]+\left(1+\frac{\vartheta_{i,j}\tau^2}{12}\delta_x^2+\frac{\vartheta_{i,j}\tau^2}{12}\delta_y^2\right)\left[\vartheta_{i.j}\left(\frac{\partial^2u}{\partial y^2}\right)_{i,j}^n\right]\\&+\left(1+\frac{\vartheta_{i,j}\tau^2}{12}\delta_x^2+\frac{\vartheta_{i,j}\tau^2}{12}\delta_y^2\right)f\left(u_{i,j}^n\right)+\frac{1}{12}\left[f\left(4u_{i,j}^n-6u_{i,j}^{n-1}+4u_{i,j}^{n-2}-u_{i,j}^{n-3}\right)-2f\left(u_{i,j}^n\right)+f\left(u_{i,j}^{n-1}\right)\right],\\&1\le i\le M_x-1,\ 1\le j\le M_y-1,\ 3\le n\le N-1,\end{aligned} \tag{2.19}$$

which we call HOC-II for convenience. We can apply HOC-II using Algorithm 2.

Algorithm 2:

Step 1 : $\left\{u_{i,j}^0|\left(x_i,y_j\right)\in\Omega_h\right\}$ *and* $\left\{u_{i,j}^1|\left(x_i,y_j\right)\in\Omega_h\right\}$ *can be calculated by* (1.2) *and* (2.3), *respectively*;

Step 2 : $\left\{u_{i,j}^n|\left(x_i,y_j\right)\in\Omega_h\right\}$, $(n=2,\ 3)$ *can be solved by HOC − I scheme*;

Step 3 : $\left(\frac{\partial^2u}{\partial x^2}\right)_{i,j}^n$ *and* $\left(\frac{\partial^2u}{\partial x^2}\right)_{i,j}^n$ *are calculated by* (2.12) − (2.17);

Step 4 : *Calculate* $\left\{u_{i,j}^{n+1}|\left(x_i,y_j\right)\in\Omega_h\right\}$, $(n=3,\ 4,\ \cdots,\ N-1)$ *through* (2.19);

Step 5 : *Let* $n\leftarrow n+1$, *repeat the above Step* 3 *and Step* 4 *till the time reaches the final moment, and the calculation is terminated.*

Remark 4: In the Step 3 of Algorithm 2, $\left(\frac{\partial^2 u}{\partial x^2}\right)_{i,j}^n$ and $\left(\frac{\partial^2 u}{\partial y^2}\right)_{i,j}^n$ can be calculated directly through (2.12) and (2.13) for the problems with periodic boundaries.

Remark 5: For the stability of the compact difference scheme, we give the stability range for the corresponding linear problem using discrete Fourier analysis in Appendix.

3. For the coupled sine–Gordon equations

This section discusses the generalization of the two HOC schemes derived in Section 2 for solving the following coupled sine–Gordon equations [8–11]:

$$\frac{\partial^2 u}{\partial t^2} - \left(\frac{\partial^2 u}{\partial x^2} + \frac{\partial^2 u}{\partial y^2}\right) = -\beta^2 \sin(u - w), (x, y, t) \in \Omega \times (0, T], \tag{3.1}$$

$$\frac{\partial^2 w}{\partial t^2} - \alpha^2 \left(\frac{\partial^2 w}{\partial x^2} + \frac{\partial^2 w}{\partial y^2}\right) = \sin(u - w), (x, y, t) \in \Omega \times (0, T], \tag{3.2}$$

in which $\Omega = [a_1, b_1] \times [a_2, b_2]$ and $\beta, \alpha > 0$ are constants. The initial conditions are

$$u(x, y, 0) = \varphi_1(x, y), \frac{\partial u(x, y, 0)}{\partial t} = \psi_1(x, y), (x, y) \in \Omega, \tag{3.3}$$

$$w(x, y, 0) = \varphi_2(x, y), \frac{\partial w(x, y, 0)}{\partial t} = \psi_2(x, y), (x, y) \in \Omega, \tag{3.4}$$

and the boundary conditions are

$$u(a_1, y, t) = g_{11}(y, t), u(b_1, y, t) = g_{12}(y, t), u(x, a_2, t) = l_{11}(x, t), u(x, b_2, t) = l_{12}(x, t), \tag{3.5}$$

$$w(a_1, y, t) = g_{21}(y, t), w(b_1, y, t) = g_{22}(y, t), w(x, a_2, t) = l_{21}(x, t), w(x, b_2, t) = l_{22}(x, t). \tag{3.6}$$

We use the same derivation method as for HOC-I to obtain the following difference scheme:

$$\begin{aligned}\delta_t^2 u_{i,j}^n = &\left(1 + \frac{\tau^2}{12}\delta_x^2 + \frac{\tau^2}{12}\delta_y^2\right)\left[\left(\frac{\partial^2 u}{\partial x^2}\right)_{i,j}^n + \left(\frac{\partial^2 u}{\partial y^2}\right)_{i,j}^n\right] \\ &- \beta^2\left(1 + \frac{\tau^2}{12}\delta_x^2 + \frac{\tau^2}{12}\delta_y^2 + \frac{\tau^2}{12}\delta_t^2\right)\sin\left(u_{i,j}^n - w_{i,j}^n\right),\end{aligned} \tag{3.7}$$

$$\begin{aligned}\delta_t^2 w_{i,j}^n = &\left(\alpha^2 + \frac{\alpha^4\tau^2}{12}\delta_x^2 + \frac{\alpha^4\tau^2}{12}\delta_y^2\right)\left[\left(\frac{\partial^2 w}{\partial x^2}\right)_{i,j}^n + \left(\frac{\partial^2 w}{\partial y^2}\right)_{i,j}^n\right] \\ &+ \left(1 + \frac{\alpha^2\tau^2}{12}\delta_x^2 + \frac{\alpha^2\tau^2}{12}\delta_y^2 + \frac{\tau^2}{12}\delta_t^2\right)\sin\left(u_{i,j}^n - w_{i,j}^n\right).\end{aligned} \tag{3.8}$$

The terms $u_{i,j}^1$ and $w_{i,j}^1$ can be derived as in Section 2.

In addition, we generalize HOC-II for solving the above equations. The corresponding calculation procedures are similar to the above, and are omitted for brevity.

4. Numerical experiments

This section first presents three experiments to confirm the effectiveness and accuracy of the two proposed HOC schemes. We use ADI-I and ADI-II to represent the ADI schemes in [6],

and ADI-III and ADI-IV are the difference schemes in [19] and [21], respectively. Note that the CPU time and numerical errors of these ADI schemes are calculated using the PHOEBE Solver (www.phoebesolver.com) on the same computer. Then, we simulate the motion states of a single-ring soliton and a soliton in a layered medium. The following examples are programmed in Fortran 90 and executed on a laptop with an Intel Core i7-10750H CPU@2.60GHz 2.59 GHz and 16 GB of RAM.

Definition 1. *The L_∞ and L_2 norm errors and Rate are defined as follows:*

$$L_\infty = \max_{\substack{0\le i\le M_x\\ 0\le j\le M_y}} \left|u_{i,j}^N - u\left(x_i, y_j, t_N\right)\right|, \quad L_2 = \sqrt{h_x h_y \sum_{i=0}^{M_x}\sum_{j=0}^{M_y}[u_{i,j}^N - u(x_i, y_j, t_N)]^2},$$

$$Rate = \frac{\log[L_\infty(h_1)/L_\infty(h_2)]}{\log(h_1/h_2)} \ \ or \ \ Rate = \frac{\log[L_2(h_1)/L_2(h_2)]}{\log(h_1/h_2)},$$

where $u(x_i, y_j, t_N)$ represents the analytical solution at point (x_i, y_j, t_N), $u_{i,j}^N$ represents the numerical solution at point (x_i, y_j, t_N). In contrast, we introduce $L_\infty = \max\{L_\infty(u), L_\infty(w)\}$ and $L_2 = \max\{L_2(u), L_2(w)\}$ in Tables 7 and 8.

4.1. The sine–Gordon equation with constant coefficients [6, 19, 21]

First, we consider the following nonlinear sine–Gordon equation:

$$\begin{cases} \frac{\partial^2 u}{\partial t^2} - \left(\frac{\partial^2 u}{\partial x^2} + \frac{\partial^2 u}{\partial y^2}\right) + \sin(u) = 0, & (x, y, t) \in [-7, 7]\times[-7, 7]\times(0, T], \\ u(x, y, 0) = 4\arctan\left(e^{x+y}\right), \ \frac{\partial u(x,y,0)}{\partial t} = -\frac{4e^{x+y}}{1+e^{2x+2y}}, & (x, y) \in [-7, 7]\times[-7, 7], \\ u(-7, y, t) = 4\arctan\left(e^{-7+y-t}\right), \ u(7, y, t) = 4\arctan\left(e^{7+y-t}\right), & (y, t) \in [-7, 7]\times(0, T], \\ u(x, -7, t) = 4\arctan\left(e^{x-7-t}\right), \ u(x, 7, t) = 4\arctan\left(e^{x+7-t}\right), & (x, t) \in [-7, 7]\times(0, T]. \end{cases}$$

The analytical solution is $u(x, y, t) = 4\arctan\left(e^{x+y-t}\right)$.

Tables 1–3 present the results obtained by computing Problem 4.1 with the various difference schemes. From Table 1, we can see that when the spatial steps are $1/2$, $1/2^2$, $1/2^3$ and $1/2^4$, the errors calculated by the two difference schemes are essentially the same. When the spatial steps are $1/2^5$ and $1/2^6$, the calculation errors of ADI-I are obviously larger than those of HOC-I. This is because the start-up level calculations for ADI-I have only third-order accuracy in the time direction, which does not match the fourth-order accuracy of the main difference scheme. This affects the calculation results. Furthermore, with the reduction in the spatial step size, the HOC-I scheme becomes significantly better than ADI-I in terms of computational efficiency. From Table 2, we can obtain the same conclusion. In addition, we find that HOC-II requires only half the CPU time of HOC-I to compute Problem 4.1 with the same stride length. This illustrates the importance of constructing the linearized difference scheme HOC-II. Table 3 presents the calculation results using the difference schemes in [21] and [19]. From the table, we find that the error produced by these difference schemes is greater than that calculated by the proposed method when the spatial step size is the same. The two HOC schemes described in this paper have better computational efficiency than the previous difference schemes considered here.

Table 1. Numerical results of ADI-I and HOC-I schemes with $\tau = h/3$ for Problem 4.1.

h	ADI-I Scheme [6]			HOC-I Scheme		
	L_∞	L_2	CPU	L_∞	L_2	CPU
$1/2$	1.7239E-03	5.7893E-03	0.0250	1.5806E-03	5.3049E-03	0.0090
$1/2^2$	1.1414E-04	3.3199E-04	0.1870	1.1228E-04	3.0631E-04	0.0440
$1/2^3$	6.6665E-06	2.0006E-05	1.4110	6.9646E-06	1.8959E-05	0.2270
$1/2^4$	3.3964E-07	1.4431E-06	9.9180	4.4107E-07	1.1866E-06	1.7660
$1/2^5$	3.8001E-08	1.5373E-07	77.0680	2.7658E-08	7.4327E-08	15.5420
$1/2^6$	4.6741E-09	1.9829E-08	524.1290	1.7334E-09	4.6523E-09	131.0400

Table 2. Numerical results of ADI-II and HOC-II schemes with $\tau = h/3$ for Problem 4.1.

h	ADI-II Scheme [6]			HOC-II Scheme		
	L_∞	L_2	CPU	L_∞	L_2	CPU
$1/2$	1.7176E-03	5.8031E-03	0.0120	1.5635E-03	5.2774E-03	0.0060
$1/2^2$	1.1383E-04	3.3279E-04	0.0490	1.1089E-04	3.0359E-04	0.0280
$1/2^3$	6.6563E-06	2.0073E-05	0.2190	6.8751E-06	1.8764E-05	0.1410
$1/2^4$	3.3933E-07	1.4488E-06	1.1730	4.3558E-07	1.1738E-06	0.9190
$1/2^5$	3.7968E-08	1.5410E-07	8.7540	2.7320E-08	7.3509E-08	7.2570
$1/2^6$	4.6722E-09	1.9850E-08	67.8500	1.7123E-09	4.6005E-09	56.3600

Table 3. Numerical results of ADI-III and ADI-IV schemes with $\tau = h^2$ for Problem 4.1.

h	ADI-III Scheme [21]			ADI-IV Scheme [19]		
	L_∞	L_2	CPU	L_∞	L_2	CPU
$1/2$	3.1413E-02	1.4231E-01	0.0030	3.2312E-02	1.5058E-01	0.0020
$1/2^2$	2.6796E-03	1.1024E-02	0.0180	2.5032E-03	1.0968E-02	0.0130
$1/2^3$	1.7370E-04	6.5645E-04	0.1930	1.6243E-04	7.0385E-04	0.1760
$1/2^4$	1.0949E-05	4.1275E-05	2.7520	1.0303E-05	4.4263E-05	2.7330
$1/2^5$	6.8676E-07	2.5835E-06	50.9250	6.4530E-07	2.7705E-06	50.2330
$1/2^6$	4.2952E-08	1.6154E-07	859.8550	4.0346E-08	1.7321E-07	867.9500

According to the data in these tables, we plot the corresponding L_∞ error and L_2 error convergence order graphs in Figure 1. For both the L_∞ norm and the L_2 norm, the schemes proposed in this paper have the same fourth-order convergence speed as the previously developed schemes. This also means that the proposed schemes achieve fourth-order convergence in both the temporal and spatial dimensions, which accords with their theoretical accuracy. However, the convergence accuracy of ADI-I and ADI-II decreases in the fine mesh, reflecting the effects of the convergence accuracy of the start-up level.

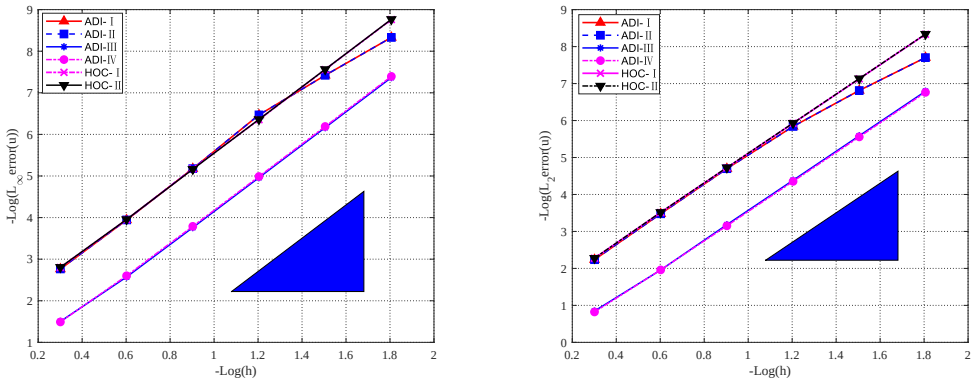

Figure 1. Log-log plots for the L_∞ and L_2 norm errors.

Furthermore, we substitute the exact solution into the source term to degenerate Problem 4.1 into a linear problem to verify the stability of difference scheme (1), and numerical results are listed in Table 4. It can be seen from Table 4 that the stability conditions we obtained through numerical experiments are consistent with the theoretical analysis.

Table 4. L_∞ errors with $h = 1/20$ for different τ and T for Problem 4.1.

τ	$v_{\max}\lambda$	$T = 20$
1/35	0.5714	1.2229E-07
1/32	0.6250	1.1468E-07
1/30	0.6667	1.1047E-07
1/29	0.6897	1.0879E-07
1/28	0.7143	6.8843E+32
1/27	0.7407	1.9898E+82

4.2. The sine–Gordon equation with periodic boundary condition [22]

Next, we consider the sine–Gordon equation with periodic boundary condition:

$$\begin{cases} \frac{\partial^2 u}{\partial t^2} - v^2(x,y)\left(\frac{\partial^2 u}{\partial x^2} + \frac{\partial^2 u}{\partial y^2}\right) + \sin(u) = f(x,y,t), & (x,y,t) \in [0,2]\times[0,2]\times(0,T], \\ u(x,y,0) = 0, \quad \frac{\partial u(x,y,0)}{\partial t} = \sin(\pi x)\sin(\pi y), & (x,y) \in [0,2]\times[0,2], \end{cases}$$

in which $v^2(x,y) = 1 + 0.1x + 0.1y$, $f(x,y,t) = 2\pi^2 t(1 + 0.1x + 0.1y)\sin(\pi x)\sin(\pi y) + \sin[t\sin(\pi x)\sin(\pi y)]$, and the analytical solution is $u(x,y,t) = t\sin(\pi x)\sin(\pi y)$.

Table 5 presents the numerical results using the HOC schemes proposed in this paper and the difference scheme in [22] under different spatial step sizes, where the time steps are $\tau = h/2$ and $\tau = h$, respectively. From the table, we can clearly see that the numerical errors calculated by the two difference schemes have little difference. Moreover, the computational results show that the proposed difference scheme achieves fourth-order convergence in both temporal and spatial dimensions for problems with variable coefficients. This agrees with our theoretical derivation and analysis. Table 6 presents the calculation results with the two difference schemes constructed in this paper. From the table, we

can see that the calculated errors are almost the same for HOC-I and HOC-II, and both have fourth-order convergence. In addition, the HOC-II scheme requires about half the CPU time of HOC-I. This demonstrates the significance of the HOC-II scheme described in this paper.

Table 5. L_2 norm error and convergence rate of different schemes at $T = 2$ for Problem 4.2.

h	EP-AVF(4)-CFD Scheme [22]		HOC-I Scheme		HOC-II Scheme	
	L_2	Rate	L_2	Rate	L_2	Rate
$1/2$	5.2619E-02	−−	5.9593E-02	−−	5.9611E-02	−−
$1/2^2$	3.3000E-03	4.00	3.3749E-03	4.14	3.3745E-03	4.14
$1/2^3$	2.0490E-04	4.01	2.0668E-04	4.03	2.0667E-04	4.03
$1/2^4$	1.2757E-05	4.01	1.2852E-05	4.01	1.2852E-05	4.01
$1/2^5$	7.9638E-07	4.00	8.0222E-07	4.00	8.0223E-07	4.00

Table 6. Numerical results of HOC-I and HOC-II schemes with $\tau = 0.001$ for Problem 4.2.

h	HOC-I Scheme					HOC-II Scheme				
	L_∞	Rate	L_2	Rate	CPU	L_∞	Rate	L_2	Rate	CPU
1/4	8.5698E-03	−−	8.5729E-03	−−	0.5820	8.5698E-03	−−	8.5729E-03	−−	0.3630
1/8	5.2375E-04	4.03	5.2270E-04	4.04	2.0490	5.2375E-04	4.03	5.2270E-04	4.04	1.2740
1/16	3.2577E-05	4.01	3.2516E-05	4.01	7.5270	3.2578E-05	4.01	3.2516E-05	4.01	4.6810
1/32	2.0337E-06	4.00	2.0299E-06	4.00	28.9990	2.0337E-06	4.00	2.0299E-06	4.00	18.0600
1/64	1.2709E-07	4.00	1.2686E-07	4.00	120.7820	1.2709E-07	4.00	1.2686E-07	4.00	72.4080

Figure 2 shows the surfaces and the contour plots of the computational results using the HOC-I scheme when $\tau = 0.01$ and $h = 0.02$. The numerical results do not oscillate. In addition, the exact solutions and numerical solutions have a high level of agreement, which means that the difference schemes in this paper have good simulation ability.

4.3. Coupled sine–Gordon equations [6, 9, 10, 35]

Consider the coupled sine–Gordon equations (3.1)–(3.6) in a square domain $[-2, 2] \times [-2, 2]$ and $t \in (0, T]$. The set of analytical solutions is

$$u(x, y, t) = \gamma \sin(2\xi), \quad w(x, y, t) = \gamma \sin(2\xi) - 2\xi,$$

in which

$$\tilde{e} = \sqrt{\frac{2(1+\beta^2\alpha^2)}{1+\beta^2}}, \quad \gamma = \frac{\beta^2}{4(\tilde{e}^2-2)\mu^2}, \quad \xi = \eta(x + y - \tilde{e}t).$$

To compare with the calculation results in Ref. [6], we take the same parameters $\alpha = \sqrt{3}$, $\beta = 0.5$, $\eta = 1.5$. The initial conditions and boundary conditions are given by the analytical solutions.

We solve this problem using the difference schemes HOC-I and HOC-II at $T = 1$. For comparison, we also derive solutions using ADI-I and ADI-II [6]. Table 7 presents the numerical results calculated

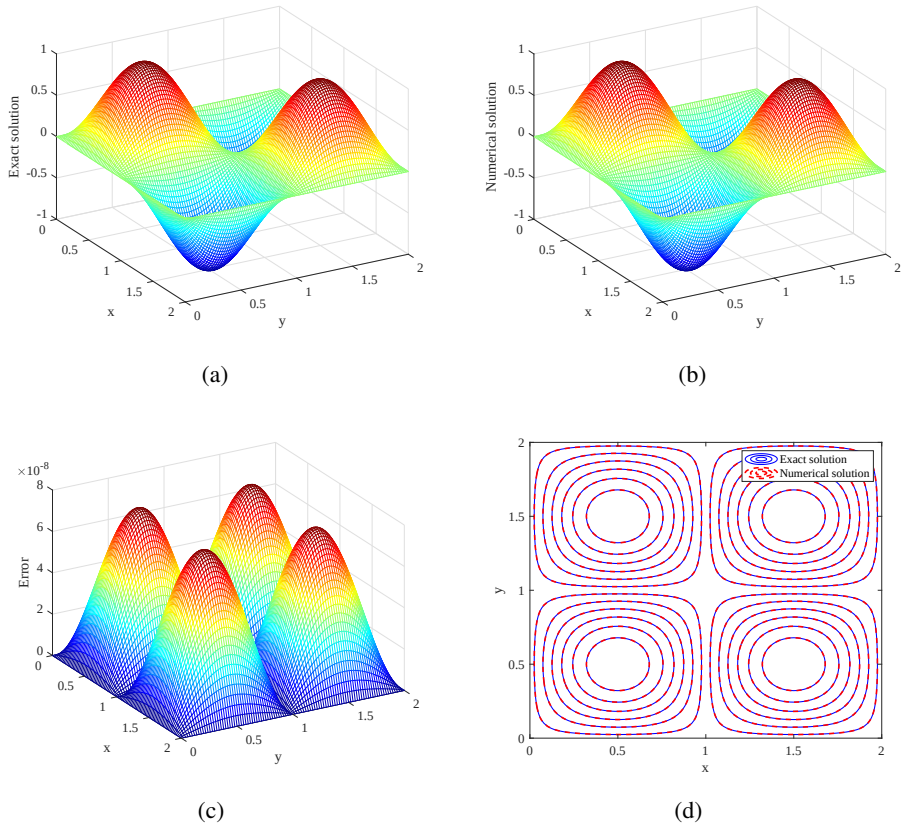

Figure 2. (a) Exact solutions, (b) numerical solutions, (c) numerical error, and (d) contour plots of the computational results with $\tau = 0.01$, $h = 0.02$, $t = 2$ for Problem 4.2.

by HOC-I and ADI-I [6]. The results using HOC-I are smaller than the values in the literature for both the L_∞ norm error and the L_2 norm error. Additionally, our schemes achieve fourth-order convergence, which is consistent with the theoretical accuracy. ADI-I does not achieve fourth-order accuracy when the spatial step sizes are $1/2^5$ and $1/2^6$, because its initial time stage has only third-order convergence instead of fourth-order convergence. In addition, the computational efficiency of HOC-I is significantly better than that of the difference scheme in the literature. Table 8 presents the calculation results for the two linearized difference schemes. Similarly, compared with ADI-II [6], the calculation results of HOC-II are better. We can also see that HOC-II is more computationally efficient than HOC-I, suggesting the superiority of the linearized HOC-II scheme.

Figure 3 shows the surfaces of the numerical solutions $u_{i,j}^n$, $w_{i,j}^n$ and the corresponding errors. From these numerical solution surfaces, we can see that the calculation results of the proposed difference scheme do not produce numerical oscillations. Therefore, the difference schemes constructed in this paper have good simulation ability.

Table 7. Numerical results of ADI-I and HOC-I schemes with $\tau = h/4$ for Problem 4.3.

h	ADI-I Scheme [6]					HOC-I Scheme				
	L_∞	Rate	L_2	Rate	CPU	L_∞	Rate	L_2	Rate	CPU
$1/2$	4.5920E-03	−−	6.2308E-03	−−	0.0050	3.6111E-03	−−	4.9899E-03	−−	0.0020
$1/2^2$	2.6343E-04	4.23	3.5686E-04	4.13	0.0350	1.9384E-04	4.22	2.7000E-04	4.21	0.0090
$1/2^3$	1.6776E-05	3.97	2.2541E-05	3.98	0.2800	1.1680E-05	4.05	1.6281E-05	4.05	0.0640
$1/2^4$	1.1225E-06	3.90	1.5562E-06	3.86	2.1150	7.2444E-07	4.01	1.0082E-06	4.01	0.4340
$1/2^5$	8.4942E-08	3.72	1.6003E-07	3.28	15.6800	4.5525E-08	3.99	6.2854E-08	4.00	3.5170
$1/2^6$	1.1453E-08	2.89	2.2850E-08	2.81	115.0570	2.8415E-09	4.00	3.9255E-09	4.00	25.1080

Table 8. Numerical results of ADI-II and HOC-II schemes with $\tau = h/4$ for Problem 4.3.

h	ADI-II Scheme [6]					HOC-II Scheme				
	L_∞	Rate	L_2	Rate	CPU	L_∞	Rate	L_2	Rate	CPU
$1/2$	4.6894E-03	−−	6.3660E-03	−−	0.0030	3.6115E-03	−−	4.9898E-03	−−	0.0010
$1/2^2$	2.7064E-04	4.11	3.6777E-04	4.13	0.0070	1.9384E-04	4.22	2.6999E-04	4.21	0.0040
$1/2^3$	1.7231E-05	3.97	2.3272E-05	3.98	0.0330	1.1681E-05	4.05	1.6283E-05	4.05	0.0260
$1/2^4$	1.1508E-06	3.90	1.6029E-06	3.86	0.1870	7.2446E-07	4.01	1.0081E-06	4.01	0.1730
$1/2^5$	8.4722E-08	3.76	1.6023E-07	3.32	1.5230	4.5525E-08	3.99	6.2854E-08	4.00	1.3000
$1/2^6$	1.1421E-08	2.89	2.2856E-08	2.81	12.3750	2.8415E-09	4.00	3.9255E-09	4.00	10.9360

4.4. Evolution of single ring soliton [6, 25, 26]

Consider the sine–Gordon equation in the square field $\Omega = [-15, 15] \times [-15, 15]$:

$$\begin{aligned}
&\frac{\partial^2 u}{\partial t^2} - \left(\frac{\partial^2 u}{\partial x^2} + \frac{\partial^2 u}{\partial y^2}\right) + sin\,(u) = 0,\\
&u\,(\mathbf{x}, 0) = 4\arctan\left(e^{3-\sqrt{x^2+y^2}}\right), \quad \frac{\partial u}{\partial t}\,(\mathbf{x}, 0) = 0, \quad \mathbf{x} \in \Omega,\\
&u\,(\mathbf{x}, t) = 0, \qquad (\mathbf{x}, t) \in \partial\Omega \times [0, T]\,.
\end{aligned}$$

The exact solution to this problem is unknown. We take time and space steps of 0.01 and 0.1, respectively, and then solve Problem 4.4 using HOC-II.

Similar to Refs. [6, 25, 26], the surfaces of $sin(U^n/2)$ at different times are shown in Figure 4, and the contours at different time are plotted in Figure 5. From Figures 4 and 5, it is apparent that the ring soliton begins to shrink at $t = 0$, before radiating and oscillating outward in a proper sequence until another ring soliton is formed at about $t = 10.5$. The next cycle of evolution then begins. There are no oscillations in these groups of figures, which proves the effectiveness and accuracy of HOC-II in solving such problems.

4.5. Evolution of double solitons in a layered medium [22]

Finally, in a layered medium covering $[-8, 8] \times [-8, 8]$, we research the following Klein–Gordon equation:

$$\frac{\partial^2 u}{\partial t^2} - v^2\left(\frac{\partial^2 u}{\partial x^2} + \frac{\partial^2 u}{\partial y^2}\right) + u + u^3 = 0,$$

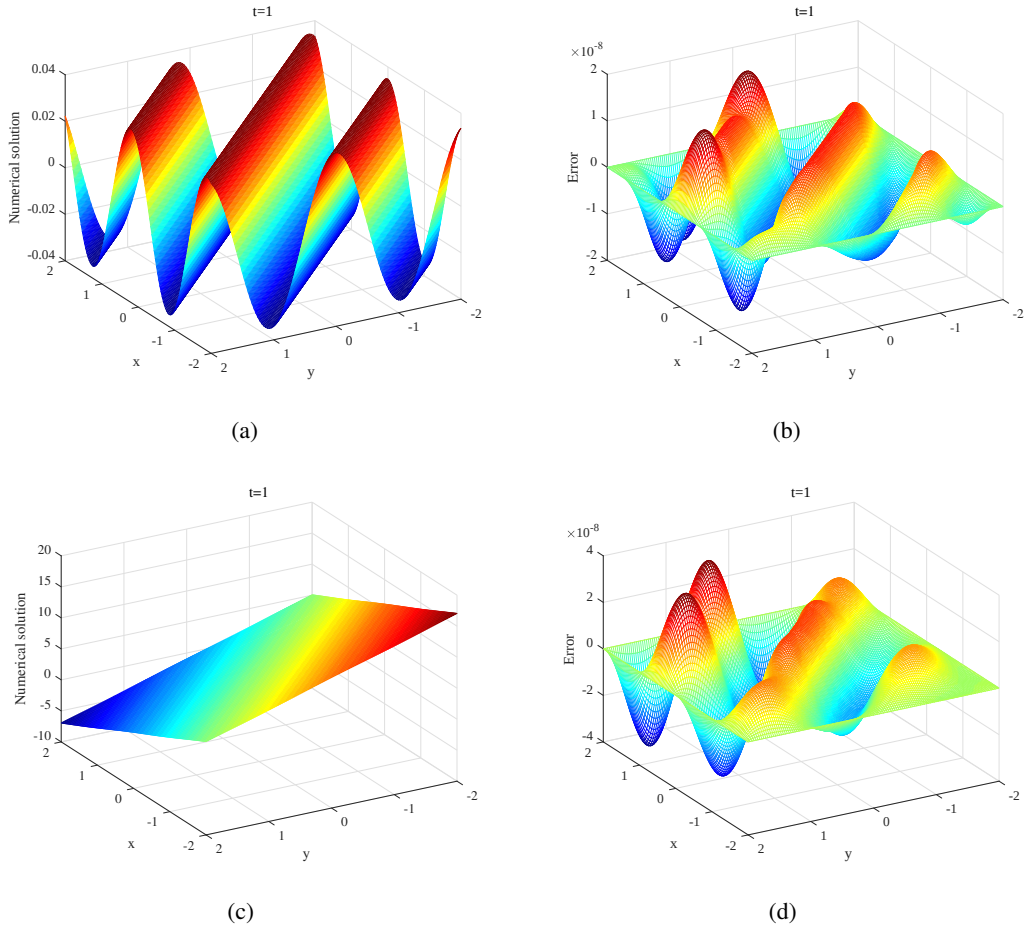

Figure 3. Surfaces of (a) numerical solution $u_{i,j}^n$ and (b) corresponding error $u_{i,j}^n - u\left(x_i, y_j, t_n\right)$; (c) numerical solution $w_{i,j}^n$ and (d) corresponding error $w_{i,j}^n - w\left(x_i, y_j, t_n\right)$ with $h = 1/32$, $\tau = 0.01$ for Problem 4.3.

in which

$$v^2 = \begin{cases} 1, & (x, y) \in [-8, 0] \times [-8, 8], \\ 0.5, & (x, y) \in (0, -8] \times [-8, 8]. \end{cases}$$

We consider periodic boundary conditions and initial conditions of

$$\begin{aligned} u(x, y, 0) =& e^{-(x+2)^2 - y^2} + e^{-(x-2)^2 - y^2}, \\ \frac{\partial u}{\partial t}(x, y, 0) =& e^{-x^2 - y^2}. \end{aligned}$$

The HOC-II scheme with time and space steps of 0.01 and 0.1 is applied to solve Problem 4.5. Figures 6 and 7 show the propagation of waves in a two-layered medium at different times. There are very complex interactions, such as contraction, radiation, and collisions between the two solitons. Furthermore, as the propagation velocity of the wave in the left medium is greater than that in the right medium, this allows us to see that the wave propagates faster in the left medium than in the right. Additionally, the greatest rate of change in u occurs at the collision center of the two solitons.

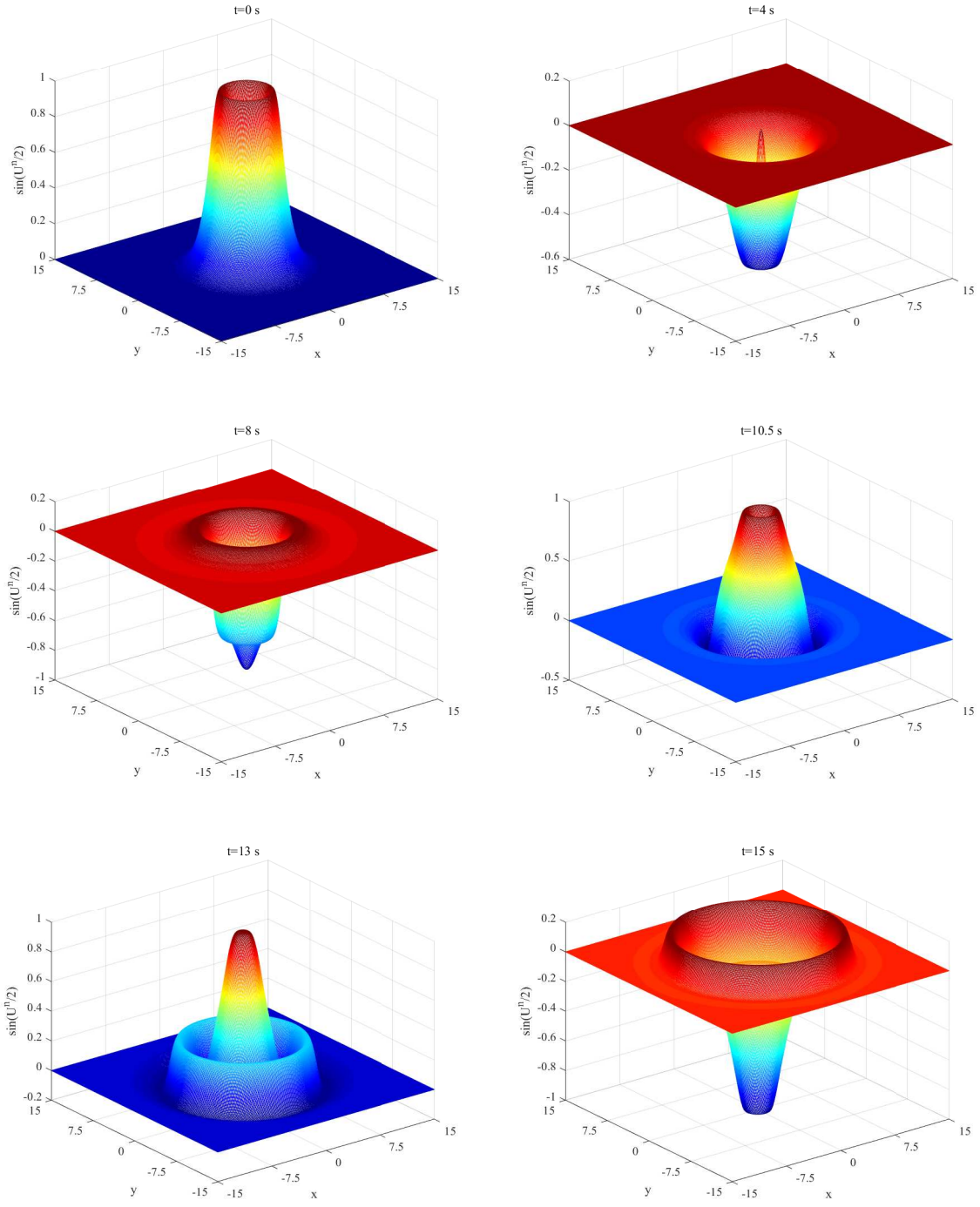

Figure 4. Surfaces of $sin(U^n/2)$ at different time t for Problem 4.4.

5. Conclusions

This paper has described the derivation of two HOC difference schemes with fourth-order accuracy for both temporal and spatial dimensions. These schemes are suitable for solving systems of the form

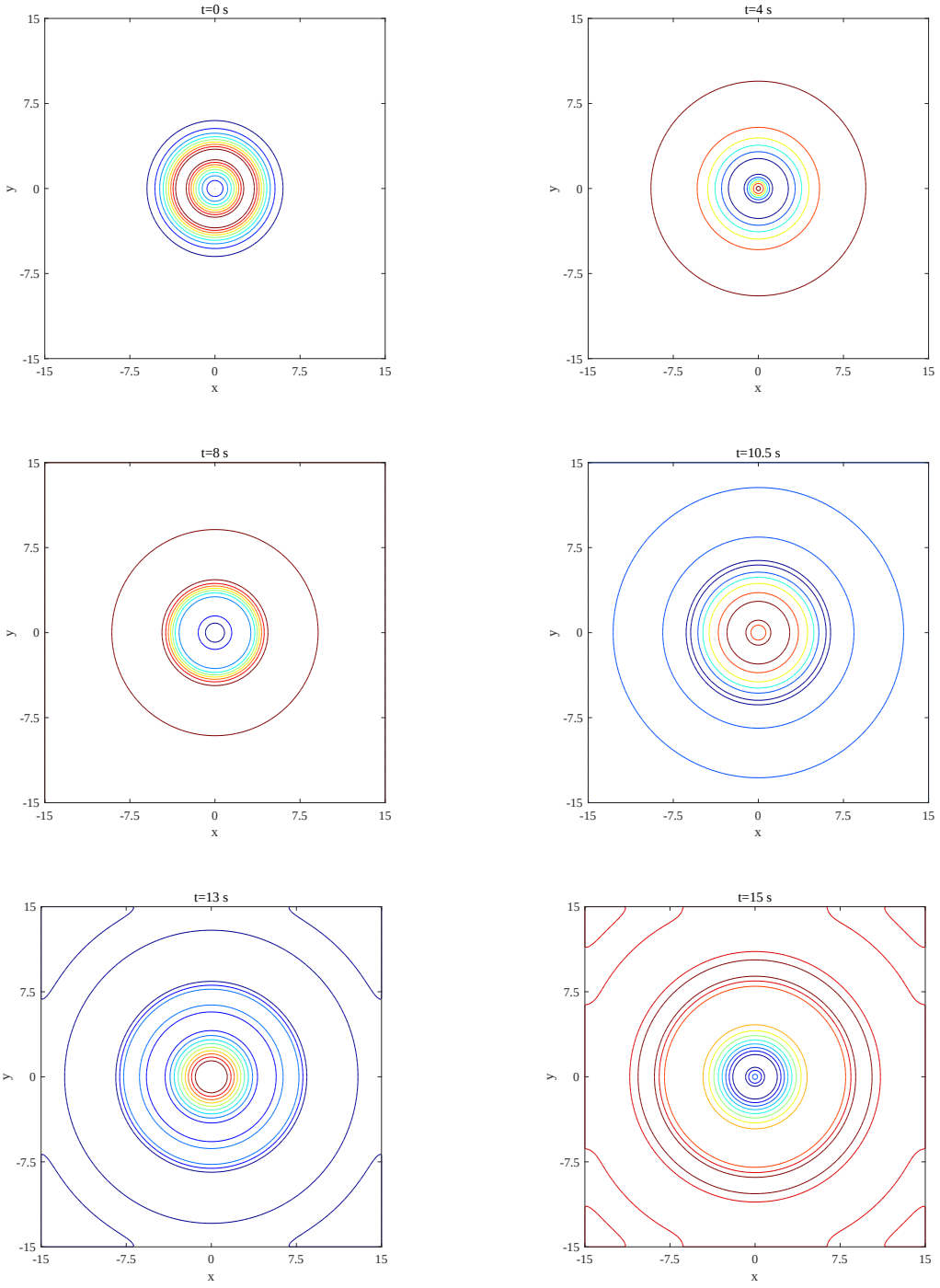

Figure 5. Contours of $sin(U^n/2)$ at different time t for Problem 4.4.

of Eqs (1.1)–(1.4). One scheme is a nonlinear fourth-order compact scheme with three temporal levels, denoted as HOC-I, and the other is a linearized fourth-order compact scheme, denoted as HOC-II. In the linear HOC-II scheme, the function value of the next time level can be directly and explicitly calculated on the premise that the spatial derivative of the previous time level has been calculated.

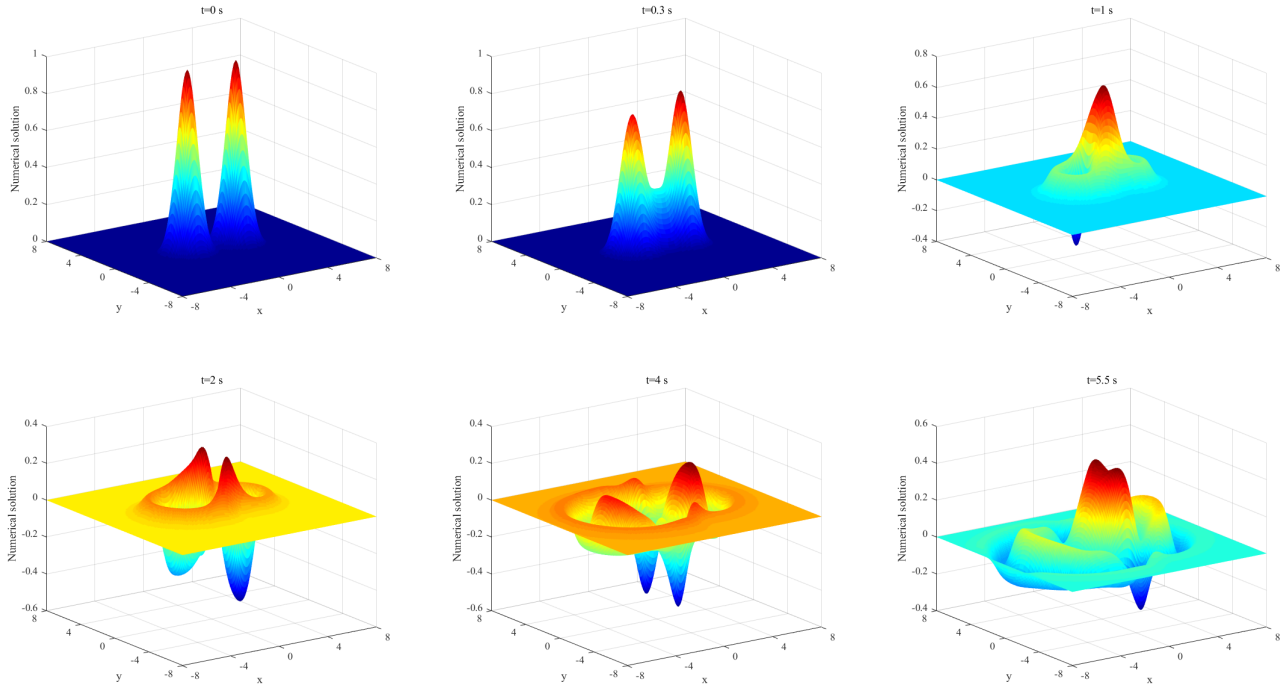

Figure 6. Surfaces of numerical solution at different time t for Problem 4.5.

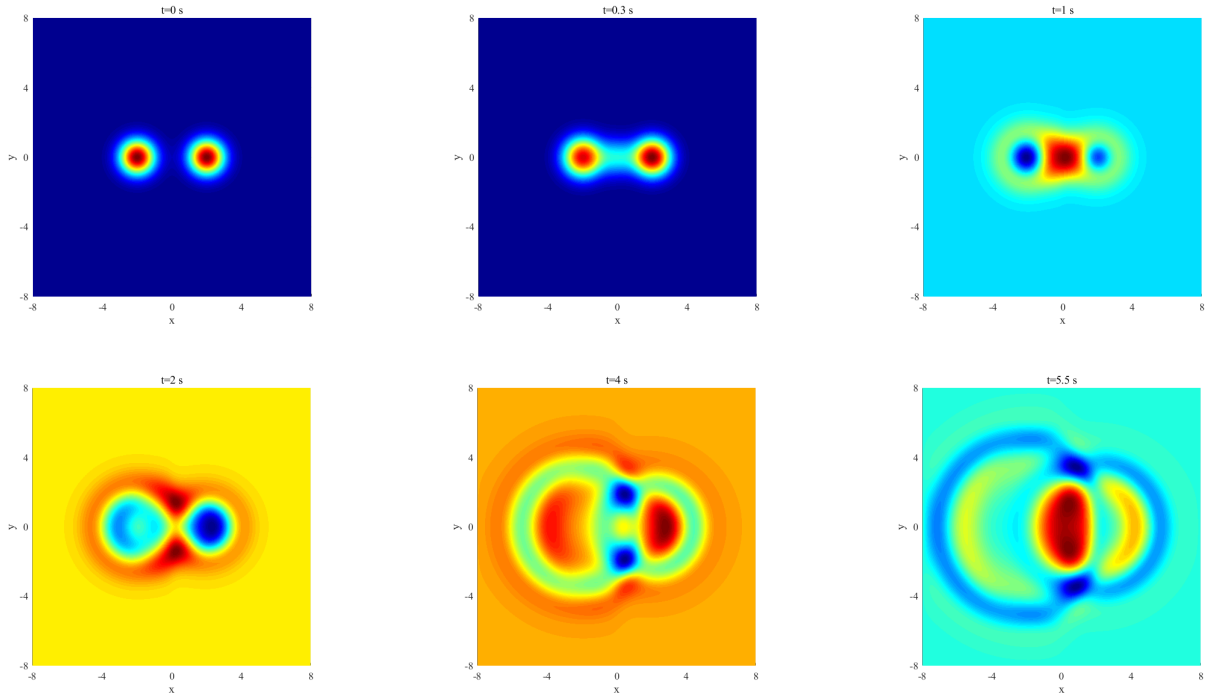

Figure 7. Planforms of numerical solution at different time t for Problem 4.5.

Therefore, we can obtain numerical solutions of acceptable accuracy at a reasonable time cost. The two fourth-order compact difference schemes proposed in this paper have been applied to simulations

of the coupled sine–Gordon equations. The accuracy and efficiency of the proposed schemes have been confirmed through a number of numerical examples, and it has been shown that HOC-II is significantly better than HOC-I and several previously developed difference schemes in terms of computational efficiency. Additionally, HOC-II has been used to simulate the motion of ring solitons and solitons in a layered medium.

In recent years, several researchers have proposed numerical methods for solving the three-dimensional wave equations and different forms of the nonlinear fourth-order wave [36–40]. The method in this paper can be extended to solve such nonlinear wave equations, and related conclusions and results will be reported in the future.

Acknowledgments

We would like to thank the editors and the referees whose constructive comments and suggestions are helpful to improve the quality of this paper. This work is partially supported by National Natural Science Foundation of China (12161067), Natural Science Foundation of Ningxia (2022AAC02023, 2020AAC03059), National Youth Top-notch Talent Support Program of Ningxia, and the First Class Discipline Construction Project in Ningxia Universities: Mathematics.

Conflicts of nterest

The authors declare no conflict of interest.

Data Availability

The data used to support the findings of this study are available from the corresponding author upon request.

Appendix. Linear stability analysis

For simplicity, the stability of the difference scheme for the linear problem is analyzed by using Fourier method. Here, we consider x- and y-directions taking the same step size, with the corresponding difference scheme as follows.

$$\begin{aligned} u_{i,j}^{n+1} &= 2u_{i,j}^{n} - u_{i,j}^{n-1} + \left(\vartheta_{i,j}\tau^2 - \frac{\vartheta_{i,j}^2\tau^2\lambda^2}{3}\right)\left[\left(\frac{\partial^2 u}{\partial x^2}\right)_{i,j}^{n} + \left(\frac{\partial^2 u}{\partial y^2}\right)_{i,j}^{n}\right] + \left(\tau^2 - \frac{\vartheta_{i,j}\tau^2\lambda_x^2}{3}\right) f_{i,j}^{n} \\ &+ \frac{\vartheta_{i,j}\tau^2\lambda^2}{12}\left[\vartheta_{i+1,j}\left(\frac{\partial^2 u}{\partial x^2}\right)_{i+1,j}^{n} + \vartheta_{i-1,j}\left(\frac{\partial^2 u}{\partial x^2}\right)_{i-1,j}^{n} + \vartheta_{i+1,j}\left(\frac{\partial^2 u}{\partial y^2}\right)_{i+1,j}^{n} + \vartheta_{i-1,j}\left(\frac{\partial^2 u}{\partial y^2}\right)_{i-1,j}^{n}\right] \\ &+ \frac{\vartheta_{i,j}\tau^2\lambda^2}{12}\left[\vartheta_{i,j+1}\left(\frac{\partial^2 u}{\partial x^2}\right)_{i,j+1}^{n} + \vartheta_{i,j-1}\left(\frac{\partial^2 u}{\partial x^2}\right)_{i,j-1}^{n} + \vartheta_{i,j+1}\left(\frac{\partial^2 u}{\partial y^2}\right)_{i,j+1}^{n} + \vartheta_{i,j-1}\left(\frac{\partial^2 u}{\partial y^2}\right)_{i,j-1}^{n}\right] \\ &+ \frac{\vartheta_{i,j}\tau^2\lambda^2}{12}\left[f_{i+1,j}^{n} + f_{i-1,j}^{n} + f_{i,j+1}^{n} + f_{i,j-1}^{n}\right] + \frac{\tau^2}{12}\left[f_{i,j}^{n+1} - 2f_{i,j}^{n} + f_{i,j}^{n-1}\right]. \end{aligned} \tag{1}$$

Lemma 2. *[41] The sufficient and necessary condition for the roots of the quadratic equation* $\mu^2 - b\mu - c = 0$ *with real coefficients to be less than or equal to 1 is* $|c| \le 1, |b| \le 1 - c$.

Theorem 1. *Assume that there is no error in the boundary and the source term, then the stability condition of difference scheme* (1) *is*

$$v_{\max}\lambda \in \left[0, \frac{\sqrt{2}}{2}\right].$$

where $v_{\max} = \max\limits_{\substack{0\le i\le M_x\\ 0\le j\le M_y}} \left|v_{i,j}\right|$ *and* $\lambda = \frac{\tau}{h}$.

Proof. Let $U_{i,j}^n = \zeta^n e^{I(\sigma_1 x_i+\sigma_2 y_j)}$, $(U_{xx})_{i,j}^n = \mu^n e^{I(\sigma_1 x_i+\sigma_2 y_j)}$ and $\left(U_{yy}\right)_{i,j}^n = \kappa^n e^{I(\sigma_1 x_i+\sigma_2 y_j)}$, where ζ, μ and κ are amplitudes, σ_1 and σ_2 are wavenumber and $I = \sqrt{-1}$. According to (2.12) and (2.13) we have

$$h^2\left[\cos\left(\sigma_1 h\right) + 5\right]\mu^n = 12\left[\cos\left(\sigma_1 h\right) - 1\right]\zeta^n, \tag{2}$$

$$h^2\left[\cos\left(\sigma_2 h\right) + 5\right]\kappa^n = 12\left[\cos\left(\sigma_2 h\right) - 1\right]\zeta^n. \tag{3}$$

Let $W_{i,j}^{n+1} = U_{i,j}^n$, $\alpha = \max\limits_{\substack{0\le i\le M_x\\ 0\le j\le M_y}} \vartheta_{i,j} = \max\limits_{\substack{0\le i\le M_x\\ 0\le j\le M_y}} v_{i,j}^2$ and assume that there is no error in the source term, (1) can be written in the following matrix form

$$\begin{aligned}
\zeta^{n+1} &= \begin{bmatrix} 2 & -1 \\ 1 & 0 \end{bmatrix}\zeta^n + \begin{bmatrix} \tau^2\alpha - \frac{\alpha^2\tau^2\lambda^2}{3} & 0 \\ 0 & 0 \end{bmatrix}(\mu^n + \kappa^n) \\
&+ \begin{bmatrix} \frac{\alpha^2\tau^2\lambda^2}{12} & 0 \\ 0 & 0 \end{bmatrix}\left[2\mu^n\cos\left(\sigma_1 h\right) + 2\kappa^n\cos\left(\sigma_1 h\right) + 2\mu^n\cos\left(\sigma_2 h\right) + 2\kappa^n\cos\left(\sigma_2 h\right)\right] \\
&= \begin{bmatrix} 2 & -1 \\ 1 & 0 \end{bmatrix}\zeta^n + \begin{bmatrix} \tau^2\alpha - \frac{\alpha^2\tau^2\lambda^2}{3} + \frac{\alpha^2\tau^2\lambda^2}{6}\left[\cos\left(\sigma_1 h\right) + \cos\left(\sigma_2 h\right)\right] & 0 \\ 0 & 0 \end{bmatrix}(\mu^n + \kappa^n) \\
&= \begin{bmatrix} 2 & -1 \\ 1 & 0 \end{bmatrix}\zeta^n + \begin{bmatrix} \tau^2\alpha + \frac{\alpha^2\tau^2\lambda^2}{6}\left[\cos\left(\sigma_1 h\right) + \cos\left(\sigma_2 h\right) - 2\right] & 0 \\ 0 & 0 \end{bmatrix}(\mu^n + \kappa^n)
\end{aligned}$$

Then, we can obtain

$$\zeta^{n+1} = G\zeta^n, \tag{4}$$

where $G = \begin{bmatrix} A & -1 \\ 1 & 0 \end{bmatrix}$ is the error propagation matrix, and $A = 2BC\alpha^2\lambda^4 + 12B\alpha\lambda^2 + 2$, $B = \frac{[\cos(\sigma_1 h)-1]}{[\cos(\sigma_1 h)+5]} + \frac{[\cos(\sigma_2 h)-1]}{[\cos(\sigma_2 h)+5]}$, $C = [\cos(\sigma_1 h) + \cos(\sigma_2 h) - 2]$. The characteristic equation corresponding to the error propagation matrix is

$$\mu^2 - A\mu + 1 = 0.$$

According to Lemma 2, the stability condition of the difference scheme is $\left|BC\alpha^2\lambda^4 + 6B\alpha\lambda^2 + 1\right| \le 1$, i.e., $-2 \le BC\alpha^2\lambda^4 + 6B\alpha\lambda^2 \le 0$.

First, consider the inequality

$$BC\alpha^2\lambda^4 + 6B\alpha\lambda^2 \le 0. \tag{5}$$

It can be easily obtained

$$0 < \alpha\lambda^2 \leq -\frac{6}{C} \leq \frac{3}{2}. \tag{6}$$

Next consider the inequality

$$BC\alpha^2\lambda^4 + 6B\alpha\lambda^2 + 2 \geq 0. \tag{7}$$

Likewise, inequality (7) holds true when $\cos(\sigma_1 h) = \cos(\sigma_2 h) = 1$. Otherwise, let quadratic function $F(\omega) = \omega^2 BC + 6B\omega + 2$. Since $BC > 0$, the two roots of quadratic function are

$$\omega_{1,2} = -\frac{3}{C} \pm \sqrt{\frac{9}{C^2} - \frac{2}{BC}}.$$

Further analysis shows that the smallest root of the quadratic equation is 1/2. Hence, the solution satisfying the inequality (7) is

$$\alpha\lambda^2 \in [0, 1/2]. \tag{8}$$

Combining (6) and (8), the stability condition of the difference scheme (1) is $\left[0, \frac{\sqrt{2}}{2}\right]$. This completes the proof. □

References

1. A. Biswas, Soliton perturbation theory for phi-four model and nonlinear Klein-Gordon equations, *Commun. Nonlinear Sci. Numer. Simul.*, **14** (2009), 3239–3249. http://dx.doi.org/10.1016/j.cnsns.2008.12.020
2. Y. Sun, New exact traveling wave solutions for double sine-Gordon equation, *Appl. Math. Comput.*, **258** (2015), 100–104. http://dx.doi.org/10.1016/j.amc.2015.02.002
3. R. Jiwari, S. Pandit, R. C. Mittal, Numerical simulation of two-dimensional sine-Gordon solitons by differential quadrature method, *Comput. Phys. Commun.*, **183** (2012), 600–616. http://dx.doi.org/10.1016/j.cpc.2011.12.004
4. S. I. Abdelsalam, M. M. Bhatti, Anomalous reactivity of thermo-bioconvective nanofluid towards oxytactic microorganisms, *Appl. Math. Mech.*, **41** (2020), 711–724. http://dx.doi.org/10.1007/s10483-020-2609-6
5. S. I. Abdelsalam, M. Sohail, Numerical approach of variable thermophysical features of dissipated viscous nanofluid comprising gyrotactic micro-organisms, *Pramana-J. Phys.*, **94** (2020), 67. http://dx.doi.org/10.1007/s12043-020-1933-x
6. D. Deng, D. Liang, The time fourth-order compact ADI methods for solving two-dimensional nonlinear wave equations, *Appl. Math. Comput.*, **329** (2018), 188–209. http://dx.doi.org/10.1016/j.amc.2018.02.010
7. A. D. Jagtap, On spatio-temporal dynamics of sine-Gordon soliton in nonlinear non-homogeneous media using fully implicit spectral element scheme, *Appl. Anal.*, **100** (2021), 37–60. http://doi.org/10.1080/00036811.2019.1588961

8. K. R. Khusnutdinova, D. E. Pelinovsky, On the exchange of energy in coupled Klein-Gordon equations, *Wave Mot.*, **38** (2003), 1–10. http://dx.doi.org/10.1016/S0165-2125(03)00022-2

9. S. Yomosa, Soliton excitations in deoxyribonucleic acid (DNA) double helices, *Phys. Rev. A*, **27** (1983), 2120–2125. http://dx.doi.org/10.1103/PhysRevA.27.2120

10. A. H. Salas, Exact solutions of coupled sine-Gordon equations, *Nonlinear Anal. RWA*, **11** (2010), 3930–3935. http://dx.doi.org/10.1016/j.nonrwa.2010.02.020

11. O. Braun, Y. Kivshar, The Frenkel-Kontorova Model, *Springer Press*, 2003. http://doi.org/10.1007/978-3-662-10331-9

12. A. M. Wazwaz, The tanh and the sine-cosine methods for compact and noncompact solutions of the nonlinear Klein-Gordon equation, *Appl. Math. Comput.*, **167** (2005), 1179–1195. http://dx.doi.org/10.1016/j.amc.2004.08.006

13. A. M. Wazwaz, Exact solutions for the generalized sine-Gordon and the generalized sinh-Gordon equations, *Chaos. Soliton. Fract.*, **28** (2006), 127–135. http://dx.doi.org/10.1016/j.chaos.2005.05.017

14. T. Aktosun, F. Demontis, C. V. Der Mee, Exact solutions to the sine-Gordon equation, *J. Math. Phys.*, **51** (2010), 123521. http://dx.doi.org/10.1063/1.3520596

15. Q. Zhou, M. Ekici, M. Mirzazadeh, A. The investigation of soliton solutions of the coupled sine-Gordon equation in nonlinear optics, *J. Morden Opt.*, **64** (2017), 1677–1682. http://dx.doi.org/10.1080/09500340.2017.1310318

16. Y. Chen, Z. Yu, L. Zou, The lump, lump off and rogue wave solutions of a (2 + 1)-dimensional breaking soliton equation, *Nonlinear Dyn.*, **111** (2023), 591–602. https://doi.org/10.1007/s11071-022-07823-7

17. B. Dong, Z. Ye, X. Zhai, Global regularity for the 2D boussinesq equations with temperature-dependent viscosity, *J. Math. Fluid Mech.*, **22** (2020), 2. https://doi.org/10.1007/s00021-019-0463-0

18. B. Dong, Z. zhang, Global regularity of the 2D micropolar fluid flows with zero angular viscosity, *J. Differ. Equ.*, **249** (2010), 200–213. https://doi.org/10.1016/j.jde.2010.03.016

19. M. Cui, High order compact alternating direction implicit method for the generalized sine-Gordon equation, *J. Comput. Appl. Math.*, **235** (2010), 837–849. http://dx.doi.org/10.1016/j.cam.2010.07.016

20. S. Xie, S. Yi, T. I. Kwon, Fourth-order compact difference and alternating direction implicit schemes for telegraph equations, *Comput. Phys. Commun.*, **183** (2012), 552–569. http://dx.doi.org/10.1016/j.cpc.2011.11.023

21. D. Deng, C. Zhang, A new fourth-order numerical algorithm for a class of nonlinear wave equations, *Appl. Numer. Math.*, **62** (2012), 1864–1879. http://dx.doi.org/10.1016/j.apnum.2012.07.004

22. B. Hou, D. Liang, The energy-preserving time high-order AVF compact finite difference scheme for nonlinear wave equations in two dimensions, *Appl. Numer. Math.*, **170** (2021), 298–320. http://dx.doi.org/10.1016/j.apnum.2021.07.026

23. J. Argyris, M. Haase, J. C. Heinrich, Finite element approximation to two-dimensional sine-Gordon solitons, *Comput. Methods Appl. Mech. Eng.*, **86** (1991), 1–26. http://dx.doi.org/10.1016/0045-7825(91)90136-T

24. D. Shi, L. Pei, Nonconforming quadrilateral finite element method for a class of nonlinear sine-Gordon equations, *Appl. Math. Comput.*, **219** (2013), 9447–9460. http://dx.doi.org/10.1016/j.amc.2013.03.008

25. A. G. Bratsos, The solution of the two-dimensional sine-Gordon equation using the method of lines, *J. Comput. Appl. Math.*, **206** (2007), 251–277. http://dx.doi.org/10.1016/j.cam.2006.07.002

26. A. G. Bratsos, An improved numerical scheme for the sine-Gordon equation in 2 + 1 dimensions, *Int. J. Numer. Methods Eng.*, **75** (2008), 787–799. http://dx.doi.org/10.1002/nme.2276

27. D. Deng, C. Zhang, Analysis and application of a compact multistep ADI solver for a class of nonlinear viscous wave equations, *Appl. Math. Model.*, **39** (2015), 1033–1049. http://dx.doi.org/10.1016/j.apm.2014.07.031

28. D. Deng, Unified compact ADI methods for solving nonlinear viscous and non-viscous wave equations, *Chinese J. Chem. Phys.*, **56** (2018), 2897–2915. http://dx.doi.org/10.1016/j.cjph.2018.09.025

29. M. Ilati, M. Dehghan, The use of radial basis functions (RBFs) collocation and RBF-QR methods for solving the coupled nonlinear sine-Gordon equations, *Eng. Anal. Bound. Elem.*, **52** (2015), 99–109. http://dx.doi.org/10.1016/j.enganabound.2014.11.023

30. D. Deng, Numerical Simulation of the coupled sine-Gordon equations via a linearized and decoupled compact ADI method, *Numer. Funct. Anal. Optim.*, **40** (2019), 1053–1079. http://dx.doi.org/10.1080/01630563.2019.1596951

31. Y. Nawaz, M. S. Arif, W. Shatanawi, A. Nazeer, An explicit fourth-order compact numerical scheme for heat transfer of boundary layer flow, *Energies.*, **14** (2021), 3396. http://dx.doi.org/10.3390/en14123396

32. A. Bourchtein, L. Bourchtein, Explicit finite difference schemes with extended stability for advection equations, *J. Comput. Appl. Math.*, **236** (2012), 3591–3604. http://dx.doi.org/10.1016/j.cam.2011.04.028

33. K. Li, W. Liao, An efficient and high accuracy finite-difference scheme for the acoustic wave equation in 3D heterogeneous media, *J. Comput. Sci.*, **40** (2020), 101063. http://dx.doi.org/10.1016/j.jocs.2019.101063

34. S. K. Lele, Compact finite difference schemes with spectral-like resolution, *J. Comput. Phys.*, **103** (1992), 16–42. http://dx.doi.org/10.1016/0021-9991(92)90324-R

35. O. M. Braun, Y. S. Kivshar, Nonlinear dynamics of the Frenkel-Kontorova model, *Phys. Rep.*, **306** (1998), 1–108. http://dx.doi.org/10.1016/S0370-1573(98)00029-5

36. G. Zhang, Two conservative and linearly-implicit compact difference schemes for the nonlinear fourth-order wave equation, *Appl. Math. Comput.*, **401** (2021), 126055. http://dx.doi.org/10.1016/j.amc.2021.126055

37. T. Achouri, T. Kadri, K. Omrani, Analysis of finite difference schemes for a fourth-order strongly damped nonlinear wave equations, *Comput. Math. Appl.*, **82** (2021), 74–96. http://dx.doi.org/10.1016/j.camwa.2020.11.012

38. T. Achouri, Conservarive finite difference scheme for the nonlinear fourth-order wave equation, *Appl. Math. Comput.*, **359** (2019), 121–131. http://dx.doi.org/10.1016/j.amc.2019.04.033

39. M. Wu, Y. Jiang, Y. Ge, An accurate and efficient local one-dimensional method for the 3D acoustic wave equation, *Demonstr. Math.*, **55** (2022), 528–552. http://doi.org/10.1515/dema-2022-0148

40. K. Li, W. Liao, An efficient and high accuracy finite-difference scheme for the acoustic wave equation in 3D heterogeneous media, *J. Comput. Sci.*, **40** (2020), 101063. http://doi.org/10.1016/j.jocs.2019.101063

41. D. Yang, Iterative Solution for Large Linear System, 1st edition, *Academic Press*, 1971. http://doi.org/10.1016/C2013-0-11733-3

AIMS Press